Self-Regularization of Chaos in Neural Systems: Experimental and Theoretical Results

Mikhail I. Rabinovich, Henry D. I. Abarbanel, Ramón Huerta, Rob Elson, and Al I. Selverston

***Abstract*— The results of neurobiological studies in both vertebrates and invertebrates lead to the general question: How is a population of neurons, whose individual activity is chaotic and uncorrelated able to form functional circuits with regular and stable behavior? What are the circumstances which support these regular oscillations? What are the mechanisms that promote this transition? We address these questions using our experimental and modeling studies describing the behavior of groups of spiking-bursting neurons. We show that the role of inhibitory synaptic coupling between neurons is crucial in the self-control of chaos.**

***Index Terms*— Chaos, neural assemblies, self-control, synaptic coupling.**

I. Introduction

A. The Problem

IT NO LONGER seems surprising that a completely deterministic, relatively simple dynamical system is able to exhibit complex, irregular, and unpredictable temporal behavior. While one still must carefully examine irregular appearing time series to assure oneself that deterministic orbits are present, this has become straightforward. A much more challenging issue is the apparent self-organization which transpires in some networks of such chaotic elements. How is it possible for complex systems with a large number of degrees of freedom to produce regular patterns and regular rhythms. This phenomenon is frequently encountered in biological systems where chaotic elements work together to produce functional activity associated with living animals and directed responses to sensory inputs which produce cooperative motor functions. In this paper, we identify some of the ingredients which lead to this regulation of chaotic action of individual neurons. Our approach is a mixture of experimental analysis of selected subsets of familiar central pattern generators (CPG's) in invertebrate preparations and theoretical analysis of these neural assemblies using simple deterministic, chaotic models. These models are established by our earlier studies of chaotic behavior in individual neurons from these CPG's.

It has only recently been demonstrated that many oscillating neurons are dynamical systems operating in a regime which possesses low-dimensional strange attractors [1]–[6]. The experimental studies and many additional modeling studies listed above merely demonstrate that the behavior of individual neurons which are part of small and large neural assemblies generate chaos. At the same time networks of neurons, as a whole, behave in a predictable fashion. Small neural networks such as CPG's produce regular rhythmic motor patterns that control muscles. An increasing number of new experiments have appeared confirming the fact that the dynamics of neuronal assemblies are more regular than that of an individual neuron [7], [8]. This also appears to be the case for neurons in the human cortex [9].

It becomes important to clarify the origin of this regular behavior of assemblies of chaotic elements because experience with other simple systems can lead us to incorrect results. Intuition gained in the analysis of systems consisting of chaotic elements coupled dissipatively such as coupled electrical oscillators, autocatalytic chemical reactions with diffusion, and so forth, suggests that the behavior of an assembly can function as a simple yet still chaotic unit [10], [11]. Indeed, electrical coupling proportional to the mismatch of the variables in coupled oscillators tends to drive the oscillators into synchrony. If the dissipative coupling is strong compared to the growth rate of spreading chaotic trajectories, then the chaotic oscillators are completely synchronized and function as a unit, and this unit can still be chaotic. For weak dissipative coupling, on the other hand, the regime of chaotic synchronization is typically unstable, and the dynamics of the coupled pair becomes more complicated. Namely, the number of positive Lyapunov exponents is doubled and the dimension of the limiting chaotic set grows. Such electrical or dissipative couplings are also encountered in biological neural networks, although, couplings through inhibitory or excitatory chemical synapses are more typical. Synaptic couplings exhibit two essential nonlinear features: threshold and saturation. These couplings significantly change the dynamics of spike-train generation and, as we will demonstrate here, may lead to a complete suppression of chaos.

Manuscript received January 23, 1997; revised May 7, 1997. The work of M. I. Rabinovich, H. D. I. Abarbanel, and R. Huerta was supported in part by the U.S. Department of Energy, Office of Basic Energy Sciences, Division of Engineering and Geosciences, under Grants DE-FG03-90ER14138 and DE-FG03-96ER14592, and in part by the Office of Naval Research (Contract N00014-91-C-0125). The work of R. Elson and A. I. Selverston was supported by the National Science Foundation under Grant IBN-9122712. This work was also supported in part by NSF Grant NCR(FDP) NCR-9612250 and Grant IBN-96334405 from the National Science Foundation. This paper was recommended by Guest Editor M. P. Kennedy.

M. I. Rabinovich and R. Huerta are with the Institute for Nonlinear Science, University of California, San Diego, La Jolla, CA 92093 USA (e-mail: rabin@gibbs.ucsd.edu; huerta@hamilton.ucsd.edu).

H. D. I. Abarbanel is with the Department of Physics and the Marine Physical Laboratory of Scripps Institution of Oceanography, University of California, San Diego, La Jolla, CA 92093 USA (e-mail: hdia@hamilton.ucsd.edu).

R. Elson and A. I. Selverston are with the Department of Biology, University of California, San Diego, La Jolla, CA 92093 USA (e-mail: relson@ucsd.edu; aselverston@ucsd.edu).

Publisher Item Identifier S 1057-7122(97)07326-1.

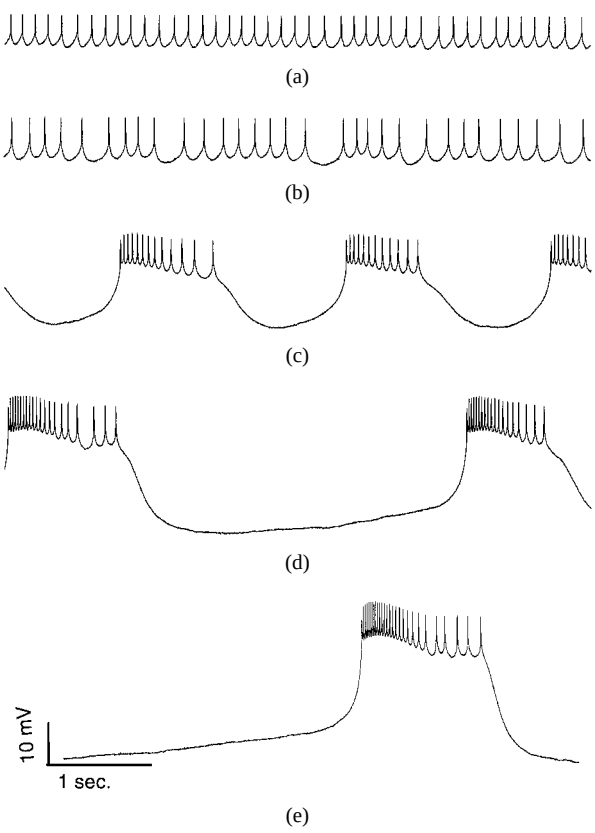

Fig. 1. Membrane potentials of the LP neuron for several values of the applied current. (a) $I = 2$ nA. (b) $I = 1$ nA. (c) $I = 0$ nA. (d) $I = -1$ nA. (e) $I = -2$ nA.

B. The Chaotic Neuron

To illustrate the chaotic features of spiking bursting neurons, we will discuss the individual dynamics of the LP neuron, from the Pyloric CPG of the California spiny lobster [8], for different values of current injected intracellularly. In order to isolate the LP neuron, the nervous system was pinned out in a Sylgard-lined dish, filled with normal lobster saline composed of NaCl 479 mM, KCl 13 mM, $CaCl_2$ 14 mM, Mg SO_4 6 mM, Na_2 SO_4 4 mM, Hepes 5 mM with a pH of 7.4. The STG was separately superfused by a continuous flow of chilled saline 14–17°C; temperature variations were kept to 1° during each recording session. For synaptic isolation of the LP neuron, we photoinactivated three presynaptic neurons (2PD's and a VD) by filling them with 5, 6-carboxyfluorescein and then illuminating with intense blue light. The remaining synaptic inputs were removed by adding of $7.5 \cdot 10^{-6}$ M of picrotoxin (PTX). The synaptically isolated LP was impaled with two microelectrodes for separate current passage and voltage recording. The observations consist of intracellular voltage taken at a data rate of 2 kHz; a time course is shown in Fig. 1. For each measurement we record approximately five minutes of real time data, and this provides a thorough view of the system attractors.

An important feature of dynamical chaos is the instability of individual trajectories in the system phase space. It is important that the action of small amounts of noise does not alter this in any significant manner. Noise transfers the motion from one trajectory to another, but these trajectories correspond to the same chaotic attractor, which is only slightly changed by the noise. Small amounts of noise can qualitatively change the properties of the orbits, if the system generating the time series is not structurally stable. To examine this issue in our neuronal samples, we reconstructed the phase portraits of the observed motion in an appropriate embedding space for different values of external applied current. These results are depicted in Fig. 2. Fig. 2(a) and (b) depict limit cycles that are topologically equivalent for different values of the current. The thickness of the attractors, which corresponds to the level of noise, does not change. Fig. 2(c)–(e) is a clear signal that we are seeing dynamical chaos because, despite the presence of the noise, the attractors have a very clear robust substructure, which is connected with the exponential instability of the trajectories. We conclude that we are not near a bifurcation boundary in these observations, so our modeling should take that into account.

C. The Model

What kind of equations are needed to reasonably represent the spiking–bursting chaotic behavior in an individual neuron? Starting from the classical Hodgkin–Huxley formulation of the dynamics of ionic channels, numerous simpler "reduced" models have been derived and extensively discussed. To capture both the bursting behavior and the spiking behavior observed in intracellular voltage measurements, one requires a combination of slow and fast subsystems acting in coordination. The fast subsystem is associated with the membrane voltage and rapid conduction channels, typically those due to Na^+ and K^+. The slow subsystem is critical for bursting behavior on top of which the spikes occur. Here we will use a three-variable Hindmarsh–Rose (HR) model [12] that describes in dimensionless units the membrane potential $x(t)$ and an auxiliary variable called $y(t)$ representing a set of fast ion channels connected with aspects of potassium and sodium transport, and finally a "slow" variable $z(t)$, which captures the slower dynamics of yet other ion channels. The choice of dimension three is not for simplicity, but this is what appears in a clean fashion from the analysis of the time course of an individual LP neuron from our CPG. This model generates time series that look like the time series of an isolated LP neuron [Fig. 1(c)], and its strange attractor has the same topology as the one depicted in Fig. 2(c). The model contains the appropriate mix of slow and fast dynamics to describe adequately the bursting and spiking behavior of observations in neural systems. The HR model is

$$\begin{aligned} \frac{dx(t)}{dt} &= y(t) + \phi[x(t)] - z(t) + I, \\ \frac{dy(t)}{dt} &= \psi[x(t)] - y(t), \\ \frac{dz(t)}{dt} &= -rz(t) + rS[x(t) - c_x] \end{aligned} \tag{1}$$

and $\phi[x(t)]$ and $\psi[x(t)]$ are determined from empirical observations on voltage–current relations

$$\begin{aligned} \phi(x) &= ax^2 - x^3 \\ \psi(x) &= 1 - bx^2 \end{aligned} \tag{2}$$

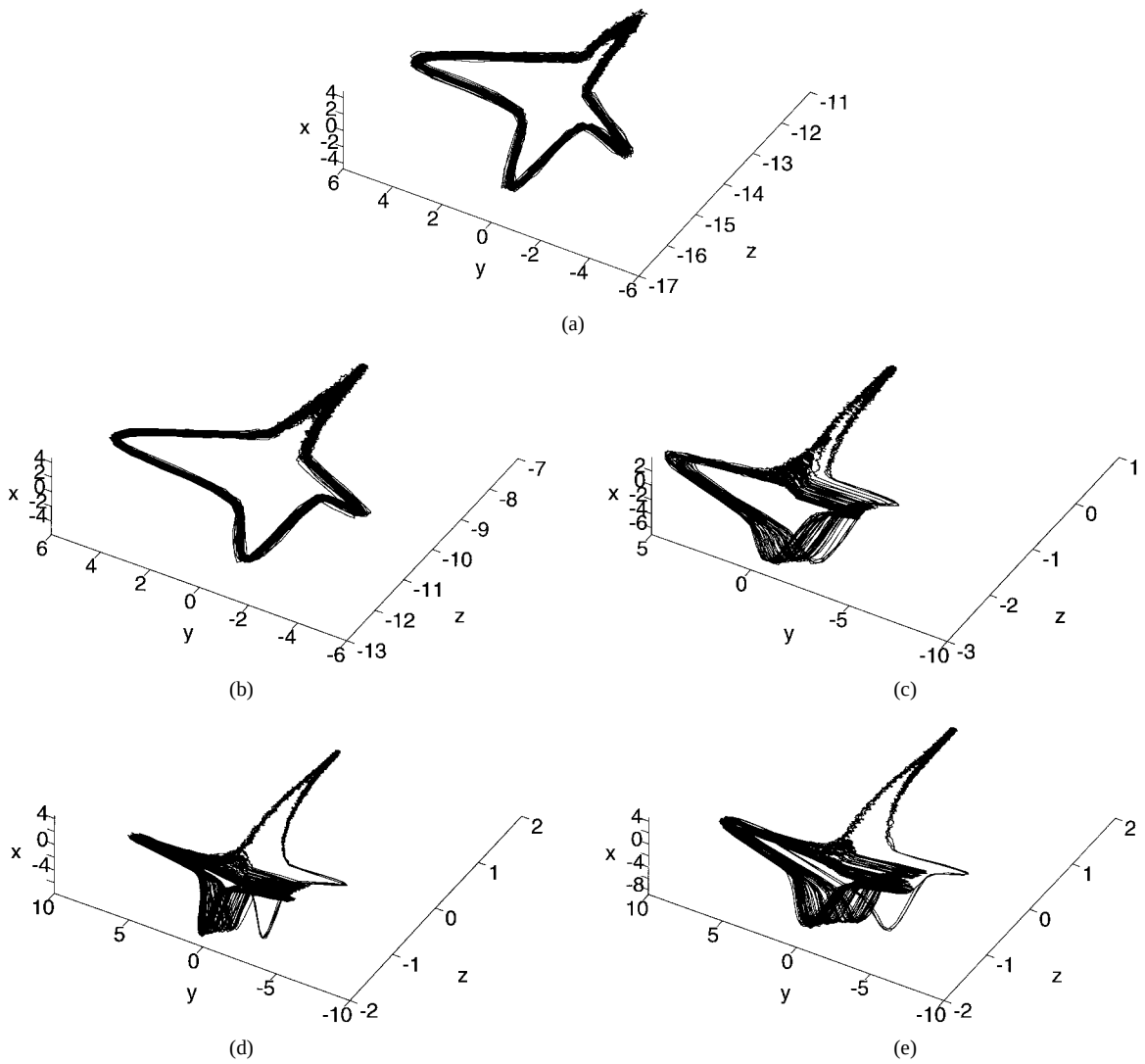

Fig. 2. State-space reconstructions from the isolated LP neuron for different values of the current. These have been obtained applying singular value decomposition to a time delay state space reconstruction using a time delay of 5 ms (see [14]). This procedure rotates and scales the original coordinates so that the fast spiking motion takes place in the plane x–y and the slow, bursting motion moves along the z axis. (a) $I = 2$ nA. (b) $I = 1$ nA. (c) $I = 0$ nA. (d) $I = -1$ nA. (e) $I = -2$ nA.

and $a = 3$, $b = 5$. The other parameters in the equations are chosen in our calculations as $I = 3.281$, $c_x = -1.6$, $S = 4$, and the scale of the influence of the membrane voltage on the slow adaptation current is $r = 0.0021$. An example of chaotic behavior for the HR neuron for these parameters is depicted in Fig. 3.

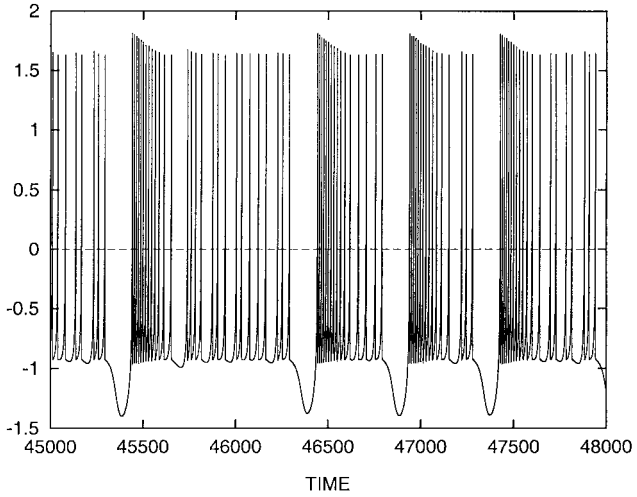

Fig. 3. Time series from an HR neuron, (1).

We now discuss aspects of the dynamics of coupled HR neurons. First, we look at synchronization between identical and then different model neurons, and following this, we consider the way synchronized chaotic neurons change the information content associated with spike number in their spike train as a combination of electrical and synaptic coupling is altered.

II. Synchronization in Two Inhibitory Coupled Model Neurons

A. Identical Neurons

In a simply organized neural circuit such as the pyloric CPG of the California lobster it has been possible to combine the results of anatomical, physiological, and modeling studies into a circuit for the CPG. The minimal basic circuit in the

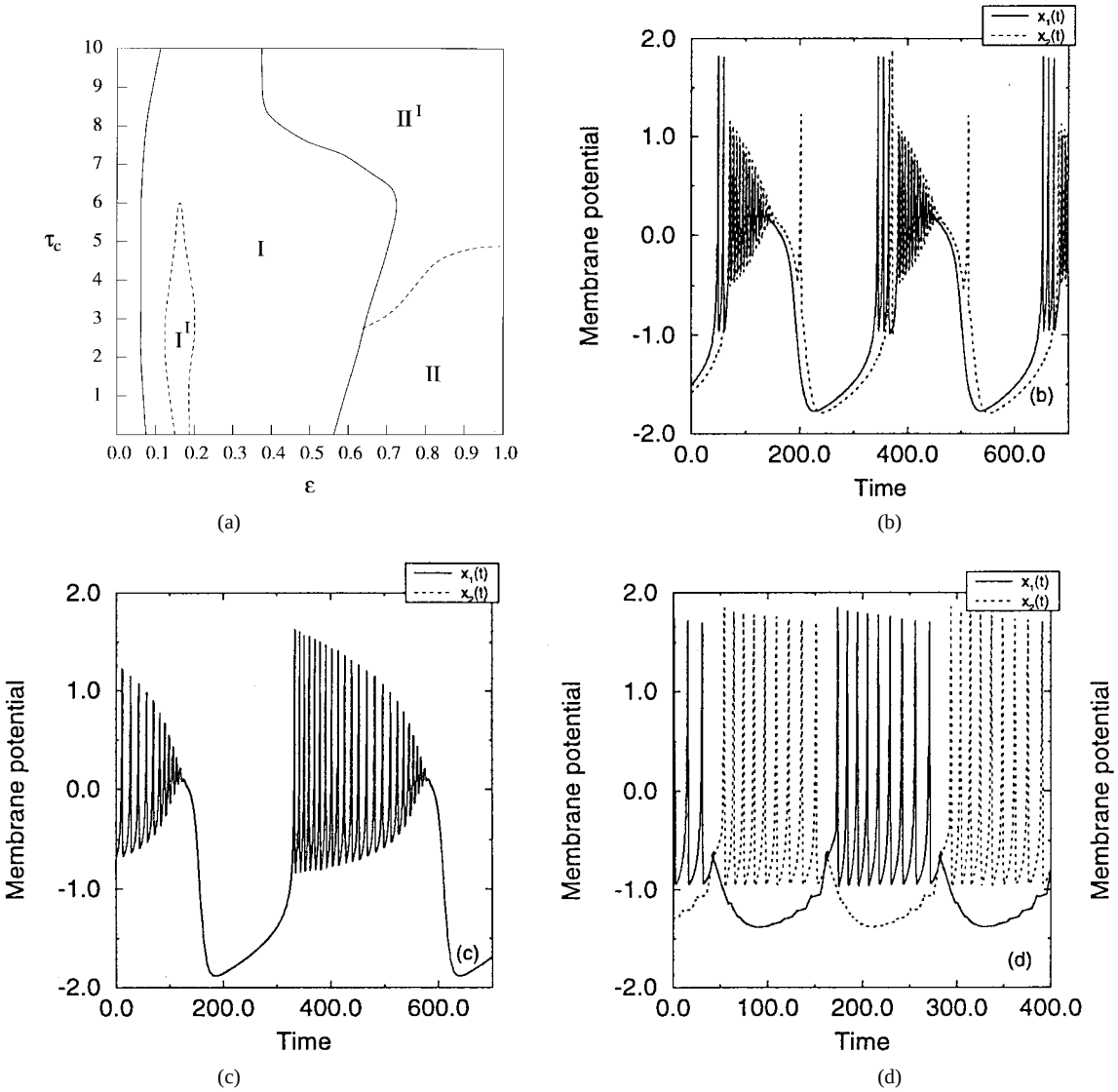

Fig. 4. (a) The "phase" diagram for inhibitory coupling between coupled HR neurons as a function of the coupling strength ϵ and the time delay τ_c in the synaptic coupling. The four labeled regions correspond to different types of synchronization illustrated by the time traces in the next figures. (b) Membrane potentials $x_1(t)$ and $x_2(t)$ in Region I. $\tau_c = 4.0$. The synchronization is nearly complete and in phase. (c) Membrane potentials $x_1(t)$ and $x_2(t)$ in Region I'. $\tau_c = 4.0$. The synchronization is complete and in phase. (d) Membrane potentials $x_1(t)$ and $x_2(t)$ in Region II. $\tau_c = 4.0$. The synchronization is complete and antiphase.

system is a pair of synaptically connected neurons. Reciprocal inhibitory coupling is the most common type in small neural networks such as CPG's. The key role in coordinating behavior and regulation of dynamics of the coupled chaotic neurons in this case belongs to chemical synapses. It is essential that the coupling between the neurons occurring in this fashion is characterized by the presence of a threshold and a constant resting potential. Consequently, in the equation describing the membrane potential x_1 of one neuron we add a synaptic current associated with the action of another neuron with potential x_2 of the form

$$-[\epsilon+\eta(t)][x_1(t)+V_c]\theta[x_2(t-\tau_c)-X]. \tag{3}$$

Here ϵ is the strength of the coupling and $\eta(t)$ is a small zero mean noise term. The threshold of synaptic action is taken into account in the Heaviside function $\theta(w)$, X is the threshold, V_s is the reverse potential, and τ_c is the synaptic delay associated with the chemical mechanism of transmission of excitation from presynaptic to postsynaptic membrane. Note that reciprocal coupling is realized through two different synapses. The basic equations for a neural network of two coupled HR neurons are

$$\begin{aligned}
\frac{dx_1(t)}{dt} &= y_1(t)+\phi[x_1(t)]-z_1(t)+I \\
&\quad -[\epsilon+\eta(t)][x_1(t)+V_c]\theta[x_2(t-\tau_c)-X] \\
\frac{dy_1(t)}{dt} &= \psi[x_1(t)]-y_1(t), \\
\frac{dz_1(t)}{dt} &= -rz_1(t)+rS[x_1(t)-c_x], \\
\frac{dx_2(t)}{dt} &= y_2(t)+\phi[x_2(t)]-z_2(t)+I \\
&\quad -[\epsilon+\eta(t)][x_2(t)+V_c]\theta[x_1(t-\tau_c)-X],
\end{aligned}$$

$$\frac{dy_2(t)}{dt} = \psi[x_2(t)] - y_2(t)$$
$$\frac{dz_2(t)}{dt} = -rz_2(t) + rS[x_2(t) - c_x]. \quad (4)$$

Our simulations of these coupled neurons had inhibitory, synaptic coupling using $X = 0.85$, $V_c = 1.4$, and $c_x = -1.6$. The computations were performed at small values of η, and the system (4) continues to show finite-dimensional behavior. Typical results of our calculations are shown in Fig. 4(a)–(d) and exhibit a remarkable phenomenon: inhibitory synaptic coupling regularizes the behavior of individual chaotic neurons through most of the region of variation of control parameters. The exception is for very weak coupling.

B. Different Neurons

What happens when the symmetry of the pair of neurons is broken? To answer this question requires an increase in the number of parameters to be explored. We have examined an example of two HR model neurons with different internal parameters that are coupled reciprocally by inhibitory synapses of different strengths. The parameters of the HR neurons are set so that they have a time scale about a factor of two with respect to each other, and the coupling strengths were $\epsilon_1 = 0.6$ and $\epsilon_2 = 1.4$ for the two synapses. In Fig. 5(a) and (b), we have the time courses of the individual model neurons, and it is clear they act rather differently. When they are coupled as indicated, they synchronize as we see in Fig. 5(c). Such robustness of this phenomenon is very important if we are to consider it as the mechanism for coherent cooperative behavior in networks of neurons that might well be different individually.

C. Optimal Control Direction in the Parameter Space

Next, we discuss the variation of the dynamics of a neural couple inside the synchronization regime as we vary the strength of the electrical and synaptic couplings. We work with two identical, coupled model neurons which interact through both electrical and reciprocal, inhibitory coupling. Such couplings are found in the gastric mill CPG of the California lobster [8]. Each model neuron is an HR oscillator, and the differential equations of the coupled system are the same as in (4) with a smoother version of the inhibitory coupling of strength ϵ_i and an electrical coupling $\epsilon_e[x_1(t) - x_2(t)]$.

These coupled neurons produce limit cycles with varying numbers of spikes on top of each burst. We call P_k the periodic trajectory corresponding to the regime with k spikes per burst and $\epsilon_k^{(L,R)}$ the left and right boundaries in ϵ_i of the region $\epsilon_k^{(L)}(\epsilon_e) < \epsilon_i < \epsilon_k^{(R)}(\epsilon_e)$ where the cycle P_k is stable. A pair of stability multipliers $[\mu_k^{(L)}, \mu_k^{(R)}]$ is connected to every cycle P_k and indicates the kind of bifurcation at the points $(\epsilon_k^L, \epsilon_k^R)$. The condition $\mu_k^{(R,L)} = +1$ determines a saddle-node bifurcation and the condition $\mu_k^{(R,L)} = -1$ determines a flip bifurcation. A codimension 1 saddle-node bifurcation results when one multiplier crosses the complex unit circle at $+1$, which means that a stable and an unstable limit cycle merge together to annihilate; see Fig. 6 for an example.

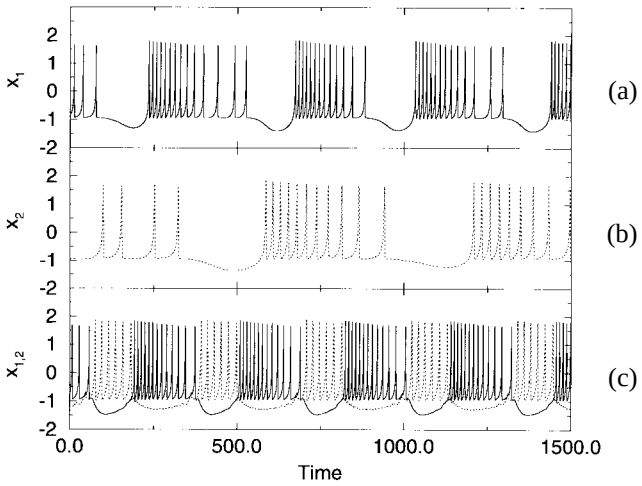

Fig. 5. (a), (b) Time series of two different HR neurons. The time scale for the neuron in (a) is half that for the neuron in (b). In (a) $r = 0.0021$ and for (b) $r = 0.0025$. (c) The time course of each of the neurons when they are coupled in a nonsymmetric fashion with reciprocal inhibitory coupling. They are now synchronized and out of phase.

How does the simplest CPG under investigation behave when some disturbance forces it to change its rhythm? The joint action of the electrical and inhibitory coupling must cooperate in an optimal way to modify any desired behavior. The results obtained from the bifurcation studies suggest that such way exists [15]. There are directions in (ϵ_e, ϵ_i) space which are perpendicular to the bifurcation lines and lead to a stronger variation in the system for the same quantitative change of the control parameters. It is important that there is no need to calculate the multipliers of the limit cycles to estimate the directions of the maximum variation. We suggest here a measure of the distance between limit cycles of close by dynamical systems; that is systems related by small perturbations of their parameters. This measure of the distance will be used to quantify the direction of the variation of the parameters in (ϵ_e, ϵ_i) space that achieves a maximal change of the limit cycle. We can define a distance between the limit cycle for a particular value of ϵ_i^* with no electrical coupling and a limit cycle for any small value of ϵ_e. We denote by $\mathbf{x}^*(t, \epsilon_i^*, 0)$ a solution corresponding to the limit cycle for $\epsilon_e = 0$ and by $\mathbf{x}(t, \epsilon_i^*, \epsilon_e)$ a solution of the limit cycle for inhibitory coupling ϵ_i and electrical coupling ϵ_e. The distance between these two trajectories is defined by

$$l(r, \theta) = \int_0^T |\mathbf{x}(t, \epsilon_i^* + r\cos\theta, r\sin\theta) - \mathbf{x}^*(t, \epsilon_i^*, 0)|^2\, dt \quad (5)$$

where T is the period of the limit cycle $\mathbf{x}^*(t, \epsilon_i^*, 0)$ and $\mathbf{x}[0, \epsilon_i^* + r\cos\theta, r\sin(\theta)]$ is reset to the nearest point of $\mathbf{x}(t, \epsilon_i^* + r\cos\theta, r\sin\theta)$ to $\mathbf{x}^*(0, \epsilon_i^*, 0)$. That is, both solutions of the limit cycles in the functional (5) are set to the same phase.

In Fig. 7, we display $l(r, \theta) = 0.015$. We show the isodistance points according to (5). The direction which gives a

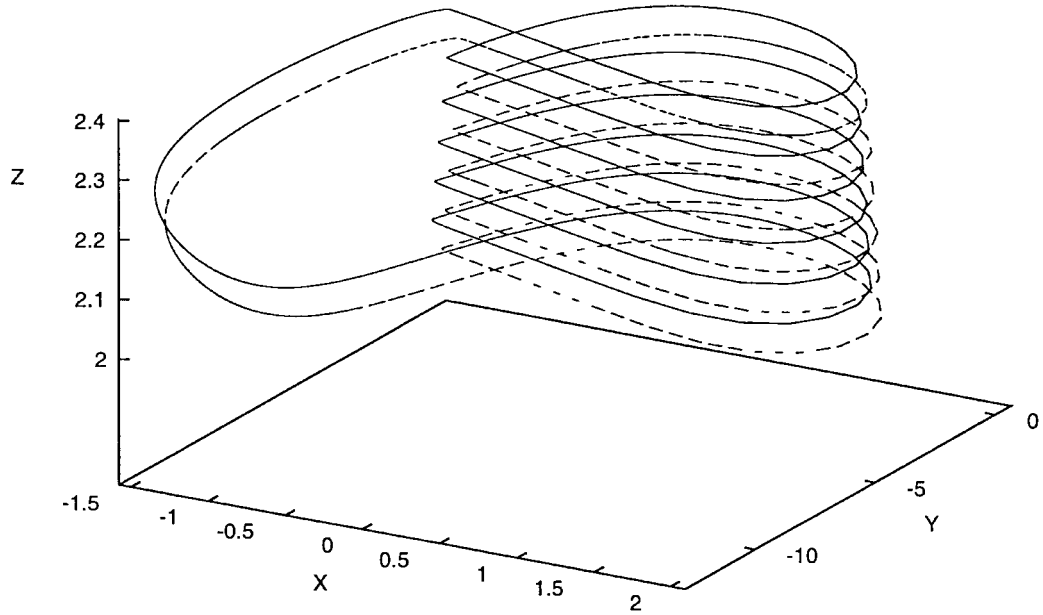

Fig. 6. Typical saddle-node bifurcation of one stable limit (solid line) and unstable limit (dashed line) cycle for two coupled Hindmarsh–Rose models. In fact, both limit cycles (stable and unstable) are very close. The distance between them has been exaggerated.

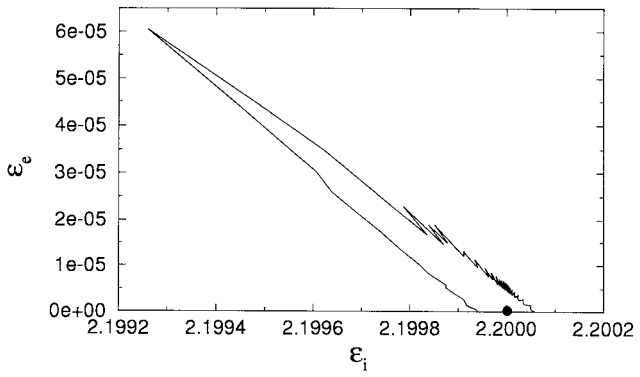

Fig. 7. Isodistance points of $l = 0.015$ starting at $\epsilon_i^* = 2.2$.

minimum variation in $l(r, \theta)$ will produce the most robust response of the coupled neurons. The perpendicular direction to the minimal variation is best way to reach a new regime. This might be a method that the CPG uses to change the mode of behavior in an optimal way with a minimum variation of the parameters.

III. Open-Loop Control in Living Neurons

A. Basic Experiments and Hypothesis

In order to understand the role of the synapse for control of chaos it is natural to measure quantitatively what happens to chaotic neurons when they are forced by an ordered signal through synaptic connections. In the pyloric CPG of lobster a special group of neurons produces a relatively regular rhythm. This is the unit composed of AB–PD neurons as in Fig. 8(a). This group is strongly electrically coupled among themselves and produce a rather regular electrical output. We measured the intracellular voltage from one of the PD cells in this unit and from the time series of voltage evaluated [16] the Lyapunov exponents associated with the dynamics. The methods require the reconstruction of a d-dimensional state space of vectors $\mathbf{y}(t)$ using time delay coordinates $\mathbf{y}(t) = \{v_{\rm PD}(t), v_{\rm PD}(t-T), \cdots, v_{\rm PD}\,[t-(d-1)T]\}$ made from the PD voltage $v_{\rm PD}(t)$ and its delays by multiples of T chosen using average mutual information. In this space, one is required to accurately estimate the Jacobians of the dynamical map taking $\mathbf{y}(t) \rightarrow \mathbf{y}(t+1) = \mathbf{F}[\mathbf{y}(t)]$. We make local polynomial maps in the reconstructed state space using cubic polynomials. The linear term in the polynomial gives the required accurate estimate of the Jacobian of the map. Diagonalizing the product of Jacobians along the observed trajectory $\mathbf{y}(t)$ yields the global Lyapunov exponents as discussed in detail in [16]. The numerically sensitive part of the calculation is the diagonalization of the ill conditioned product of Jacobian matrices; this we perform by a recursive QR decompostion. The largest exponent tells us about the predictability or regularity of the system and we found it to be $\lambda_{\rm PD} \approx 0.03$. (This is in units of an inverse sampling time for the observations.) The largest Lyapunov exponent produced by an isolated, chaotic LP neuron is five times larger than the PD neuron. In our experimental arrangement the inhibitory synaptic connection from the AB–PD unit is the only synaptic input to LP.

What can we expect of such an open-loop synaptic driving of the LP neuron? The result of the direct action of an ordered, even periodic, forcing to a chaotic oscillator depends strongly on the frequency and the waveform of the signal. Both amplitude and phase are critical in determining the response of chaotic motions to external forcing. Sometimes such a forcing is able to drive the unstable nonperiodic motions that exist between strange attractor trajectories to stable motions [17]. This is called synchronization of chaos. However these events require very special conditions. The generic result of periodic forcing of a chaotic generator is an increase of chaos:

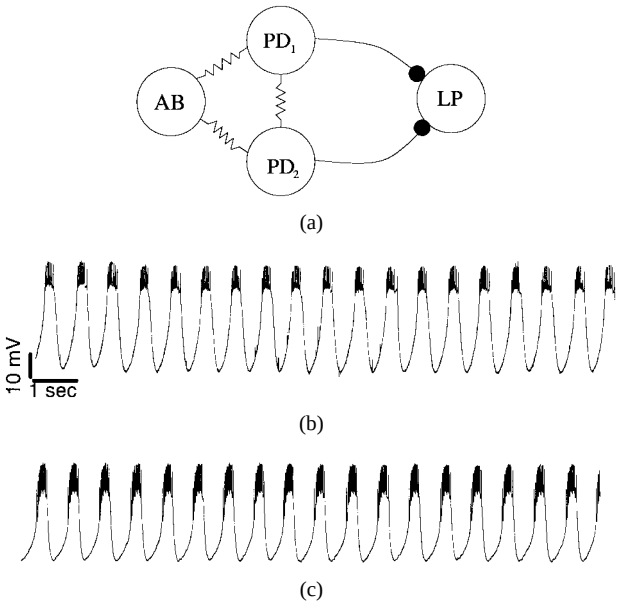

Fig. 8. (a) Diagram of the interconnections between the AB–PD unit and the LP neuron of the lobster pyloric CPG in our experiment. The VD neuron has been killed and 7.5 μm of picrotoxin has been applied throughout to suppress the inhibition from other neurons to LP. As a result the LP neuron is only inhibited by both PD neurons. (b) The membrane potential of the LP neuron under driving by the two PD neurons. The embedding dimension is $D_E = 5$, the local dimension is $D_L = 4$, the maximum Lyapunov exponent $\lambda_1 = 0.019$ and the Lyapunov dimension is $D_\lambda = 2.05$. (c) The membrane potential of one of the PD neurons inside the circuit. The embedding dimension is $D_E = 5$, the local dimension is $D_L = 4$, the maximum Lyapunov exponent $\lambda_1 = 0.037$and the Lyapunov dimension is $D_\lambda = 2.09$.

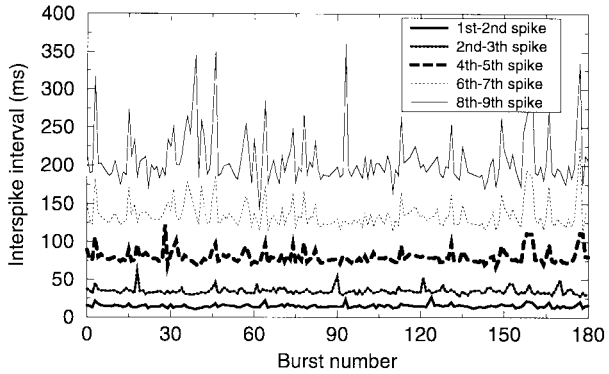

Fig. 9. Interspike interval between spike $n + 1$ and spike n in the same burst as a function of the burst number.

a few more positive Lyapunov exponents appears and a higher dimension results [18].

The result of our experiment is presented in Fig. 8(a)–(c). One can see that the LP neuron driven by PD output behaves regularly. It is important to emphasize that the same results were obtained for several experiments [19]. Quantitative measurements in the form of values of the Lyapunov exponent confirm this impression: $\lambda_{\mathrm{LP}} \approx 0.04$, which is a decrease by a factor of three from its value in isolated operation. How is the chaotic behavior of LP made more regular? The beginning of LP bursts has a more regular structure than its end as we can see in Fig. 9. Normally, synaptic inhibition from the PD neurons suppresses the irregular part of each LP burst. When the LP is inhibited, its membrane potential is driven to

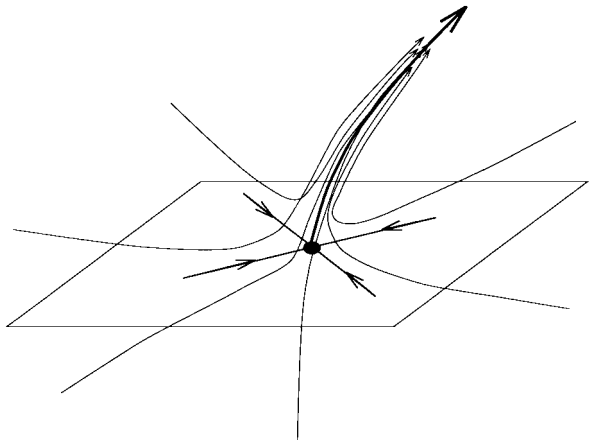

Fig. 10. Illustration of the convergence of the trajectories through a saddle-node fixed point.

about -75 mV. This hyperpolarized state is highly dissipative, causing all trajectories to converge quickly. They behave as a saddle-node fixed point (see Fig. 10) where all trajecories are brought together to the separatrix. After each hyperpolarization the membrane potential is set to very similar initial conditions and, therefore, the next burst repeats the previous one. This causes the behavior of the chaotic neuron to become rather regular. We are presently testing this hypothesis by varying the timing of action of the AB–PD group through varying injected current into the unit or by altering the chemical environment in which it operates.

B. Hybrid Experiments

The results of the previous experiments can also be used to further examine the properties of our HR neural models. We have performed a series of hybrid computations in which the model neurons are forced through an inhibitory synaptic coupling with input taken directly from the observed output of the AB–PD neural unit discussed above. The question is whether our model neuron has captured enough of the spike/burst dynamics of the ion channels comprising the actual neuron to provide the same response as the observed behavior of the LP neuron in the experiments. Using this kind of probe for the model neurons provides both a check on the models as they were formulated to describe the isolated neuron and gives us confidence that when we place these models neurons in assemblies, the behavior of the assemblies will correspond to real neurons as well.

In Fig. 11, one can see the result of the AB–PD input applied to a HR model through an inhibitory synapse. As the period of the oscillatory input is decreased, the model neuron behaves in a more regular manner. The calculation of the Lyapunov exponents confirmed this fact. In Fig. 11(f), we can compare the differences between the excitatory and inhibitory coupling through the Lyapunov exponent calculation. Small inhibition can regularize the behavior of the HR model whereas the excitation cannot. This simulation verifies the hypothesis explained in the previous section.

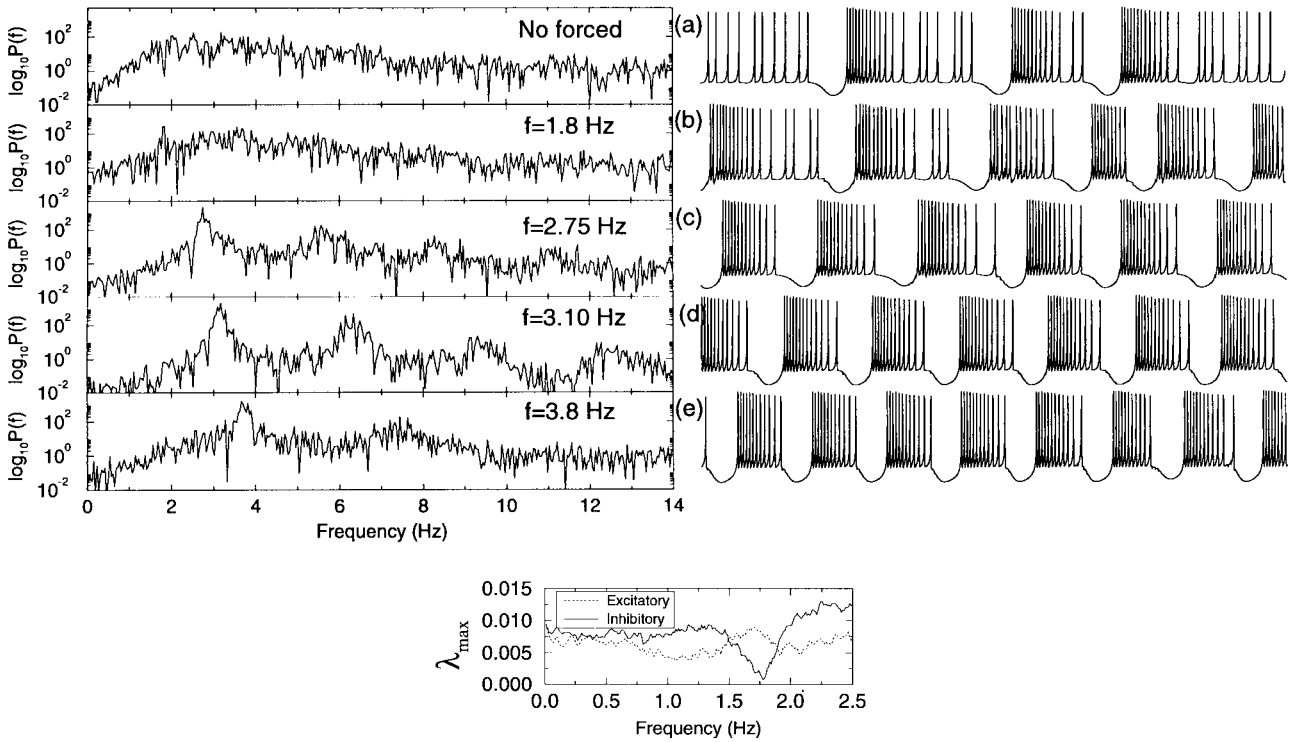

Fig. 11. An experimental time series recorded from a PD neuron is used to synaptically force a HR model. (a) Power spectra (on the left) and time series (on the right) of an isolated HR neuron. The power spectrum is flat and ranges between 1 and 8 Hz. (b) The HR neuron is forced with an experimental PD time series with frequency 2.2 Hz. The power spectrum on the left side shows how the behavior tends to be more regular but there are many other representative frequencies. (c) Forcing with 2.7 Hz the power spectrum becomes more peaked and subharmonics start appearing. (d) and (e) The forcing frequencies are around 3 Hz. These are the frequencies where the R–H model becomes more regular. (f) Lyapunov exponent calculation for inhibitory and excitatory coupling.

IV. Conclusions

Why are CPG neurons usually connected by inhibitory synapses? Standard studies of motor pattern generation do not provide an adequate answer to this question. One could build a CPG that has only excitatory synapses and nevertheless is able to produce any kind of motor pattern which the animal needs. But evolution chose inhibition. In this paper we presented the results of several different model simulations and laboratory experiments that suggest an answer to this intriguing question. We proved quantitatively that an inhibitory connection suppressed the chaotic behavior of an individual spiking–bursting neuron and consequently played a key role in producing ordered, rhythmic CPG behavior. To make the studies of the role of inhibitory connections more complete we are planning to experiment with reciprocally inhibitory coupled chaotic neurons, as well.

Here is the right place to ask the more general question: namely, why is chaos useful in nervous systems? Any neural system operates in a high dimensional state space, if only because of the myriad of ion channels influencing the dynamics. Its operation is influenced by both internal and external signals. Chaos adds a versatility to such control which simple, periodic behavior can not. When a neuron undergoes chaotic motions, it explores a much wider domain of the high dimensional space available to it than if it remained on a limit cycle during its motions. This wide ranging motion gives it immediate options in response to external and internal influences augmenting its robustness, reliability, and overall functionality. Chaotic oscillations of individual neurons may be responsible for the multitude of regular regimes of operation that can be accomplished by neuronal assemblies, and we have seen this in the simplest of neural assemblies: the pairs of coupled neurons studied in this paper. This may be a general principle by which Nature accomplishes critical functional goals.

TABLE I
Dimension and Lyapunov Exponents (in Units of the Inverse Sampling Time) for PD in the AB–PD Unit, for LP Driven by the AB–PD Unit, and for LP when Isolated

	PD	LP	Isolated LP
D_E	5	5	7
D_L	4	4	3
λ	0.019	0.037	0.1
D_λ	2.05	2.09	3.48

References

[1] K. Aihara, G. Matsumoto, and M. Ichikawa, "An alternating periodic–chaotic sequence observed in neural oscillators," *Phys. Lett. A*, vol. 111, pp. 251–255, 1985.

[2] G. J. Mpitsos, R. M. Burton, H. C. Creech, and S. S. Soinla, "Evidence for chaos in spike trains of neurons that generate rhythmic motor patterns," *Brain Res. Bull.*, vol. 21, pp. 529–538, 1988.

[3] H. Hayashi and S. Ishizuka, "Chaotic nature of bursting discharges in the Onhidium pacemaker neuron," *J. Theor. Biol.*, vol. 156, pp. 269–291, 1992.

[4] H. D. I. Abarbanel, R. Huerta, M. I. Rabinovich, N. F. Rulkov, P. F. Rowat, and A. Selverston, "Synchronized action of synaptically coupled chaotic model neurons," *Neural Computat.*, vol. 8, no. 8, pp. 1567–1602, 1996.
[5] C. C. Canavier, J. W. Clark, and J. H. Byrne, "Routes to chaos in a model of bursting neuron," *Biophys. J.*, vol. 57, pp. 1245–1251, 1990.
[6] L. Glass, *Chaos in Neural Systems. The Handbook of Brain Theory and Neural Networks*, M. Arbib, Ed. Cambridge, MA: MIT Press, 1995.
[7] G. Le Masson, S. Le Masson, and M. Moulins, "From conductances to neural network properties: Analysis of simple circuits using the hybrid network method," *Prog. Biophys. Molec. Biol.*, vol. 64, pp. 201–220, 1995.
[8] R. M. Harris-Warrick, E. Marder, A. I. Selverston, and M. Moulins, *Dynamic Biological Networks: The Stomatogastric Nervous System.* Cambridge, MA: MIT Press, 1992.
[9] G. Buzsaki, R. Llinas, R. Singer, and A. Berthoz, *Temporal Coding in the Brain: Research and Perspectives in Neurosciences.* Berlin, Germany: Springer-Verlag, 1994.
[10] V. S. Afraimovich, N. N. Verichev, and M. I. Rabinovich, "Stochastic synchronization of oscillations in dissipative systems," *Izv. VUZ.Radiofiz. RPQAEC*, vol. 29, pp. 795–803, 1986.
[11] T. L. Caroll and L. M. Pecora, "Synchronizing chaotic systems," *IEEE Trans. Circuits Syst.*, vol. 38, pp. 453–456, 1991.
[12] J. L. Hindmarsh and R. M. Rose, "A model of neuronal bursting using three coupled first order differential equations," *Proc. R. Soc. Lond. B*, vol. 221, pp. 87–102, 1984.
[13] H. D. I. Abarbanel, M. I. Rabinovich, A. Selverston, M. Bazhenov, R. Huerta, L. L. Rubchinsky, and M. M. Sushchik, "The synchronization of neural assemblies," *Uspekhi Fizicheskih Nauk*, vol. 166, no. 4, pp. 337–362, 1996.
[14] M. I. Rabinovich, A. Selverston, L. L. Rubchinsky, and R. Huerta, "Dynamics and kinematics of simple neural systems," *Chaos*, vol. 6, no. 3, pp. 288–309, 1996.
[15] R. Huerta, M. I. Rabinovich, H. D. I. Abarbanel, and M. Bazhenov, "Spike-train bifurcation scaling in two coupled chaotic neurons," *Phys. Rev. E*, vol. 55, no. 3, pp. R2108–R2110, 1997.
[16] H. D. I. Abarbanel, *Analysis of Observed Chaotic Data.* New York: Springer, 1996.
[17] H. L. Yang, Z. Q. Huang, and E. J. Ding, "Stabilization of the less stable orbit by a tiny near-resonance periodic signal," *Phys. Rev. E*, vol. 54, no. 6, pp. 889–892, 1996.
[18] A. V. Gaponov-Grekhov and M. I. Rabinovich, *Nonlinearites in Action: Oscillations, Chaos, Order, and Fractals.* New York: Springer-Verlag, 1992.
[19] R. C. Elson, R. Huerta, H. D. I. Abarbanel, M. I. Rabinovich, and A. I. Selverston, "Rhythmical inhibition regulates neural chaotic bursting in an identified neuron of an oscillatory circuit," unpublished.

Mikhail I. Rabinovich received the Ph.D. degree in physics from Nizhny Novgorod University, Russia, in 1967.

Since 1974 he has been a Full Professor of radiophysics with Nizhny Novgorod University. Currently, he is Head of the Department of Nonlinear Dynamics, Institute of Applied Physics, Russian Academy of Science, and also a Research Scientist with the Institute for Nonlinear Science, University of California, San Diego.

Dr. Rabinovich is a corresponding member of the Russian Academy of Sciences.

Henry D. I. Abarbanel, for a photograph and biography, see this issue, p. 873.

Ramón Huerta received the B.S. and M.S. degrees in physics from the Universidad Autónoma de Madrid, Spain, and the Ph.D. degree in computer science from the same University.

He is currently a Post-Doctoral Fellow at the Institute for Nonlinear Science, University of California, San Diego.

Rob Elson received the Ph.D. degree in neurobiology from the University of Cambridge, England, in 1985.

Presently, he is an Assistant Project Scientist with the Department of Biology, University of California, San Diego.

Al I. Selverston received the Ph.D. degree in biology from the University of Oregon, Eugene, in 1967.

He was a N.I.H. Post-Doctoral Fellow at Stanford University, Stanford, CA, from 1967 to 1969. From 1969 to the present, he has been a Professor with the Biology Department, University of California, San Diego.